Organic foams stabilized by Biphenyl-bridged organosilica particles

Andong Feng [a], Dmytro Dedovets [b], Yunjiao Gu [a], Shi Zhang [b], Jin Sha [a], Xia Han [c], Marc Pera-Titus [a,d,⇑]

[a] Eco-Efficient Products & Processes Laboratory (E2P2L), UMI 3464 CNRS-Solvay, Shanghai 201108, China
[b] University of Bordeaux, Laboratory of the Future (LOF), UMR 5258 CNRS-Solvay, Pessac 33600, France
[c] State Key Laboratory of Chemical Engineering, East China University of Science and Technology, Shanghai 200237, China
[d] Cardiff Catalysis Institute, School of Chemistry, Cardiff University, Main Building, Park Place, Cardiff CF10 3AT, UK

graphical abstract

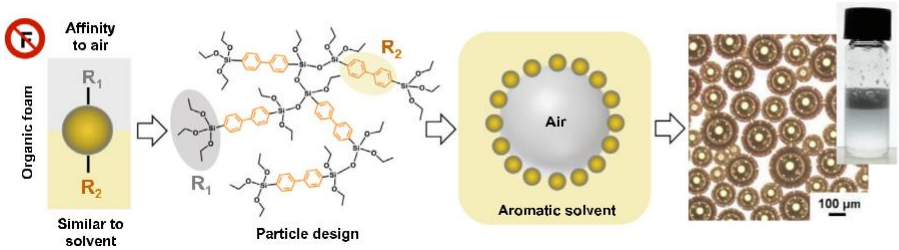

article info

Article history:

Keywords:
Non-aqueous Foam
Biphenyl-bridged
Organosilica
Contact Angle
Surface Tension

abstract

Hypothesis: Can surface-active particles be designed à la carte just by incorporating functional groups mimicking the structure of the solvent and gas? This is based on the idea that, to achieve good foamabil-ity, the particle wettability needs to be finely tuned to adjust the liquid-particle and gas-particle surface tensions. In practice, could particles containing phenyl rings and alkyl chains assemble at the air–liquid interface and stabilize foams based on aromatic solvents?

Experiments: A library of organosilica particles was prepared by sol–gel synthesis using aromatic organosilane precursors. The particles were characterized by TGA, FTIR and $^{13}C/^{29}Si$ MAS NMR. The foam-ing properties were studied after hand shaking and high-speed homogenization. The influence of particle wettability and solvent properties on foam formation was systematically investigated. A comparison was carried out between biphenyl-bridged particles and various stabilizers on foamability in benzyl alcohol. Findings: Biphenyl-bridged particles could stabilize foams in aromatic solvents with a high foam volume fraction up to 96% using Ultra-Turrax. The presence of biphenyl rings and short alkyl chains was crucial for foamability. Organic foams were prepared for aromatic solvents with intermediate surface tension (35–44 mN m ^{1}) and contact angle in the range 32–53L. Biphenyl-bridged particles outperformed poly-tetrafluoroethylene and fluorinated surfactants in benzyl alcohol.

1. Introduction

A foam is a complex system where gas bubbles are entrapped in a continuous liquid phase [1–3]. Surface-active materials such as surfactants and colloidal particles are commonly used as foaming agents and stabilizers [4–10]. In particular, the interfacial proper-ties of particles can be modified by the addition of suitable surfac-tants [11–13]. By far the most frequently and deeply studied systems are aqueous foams, which are widely used in the formula-tion of food, cosmetics, healthcare and homecare products, as well as in fire extinguishing, froth flotation and for the synthesis of por-ous materials [14–18]. In contrast, few studies have been reported on non-aqueous foams despite their importance in the cosmetic,

⇑ Corresponding author.
E-mail address: peratitusm@cardiff.ac.uk (M. Pera-Titus).

oil and manufacturing industries [19–21]. Owing to the low surface tension of organic solvents (typically ranging from 14 to 50 mN m ^{1}), the adsorption of common foam stabilizers at the gas–liquid interface is energetically unfavorable, and requires sta-bilizers with low surface energy (e.g., fluorinated surfactants), asphaltenes or fatty acid crystals [22–28]. As a result, the genera-tion of non-aqueous foams is much more challenging compared to aqueous foams [26,29].

Particle adsorption at the gas–liquid interface depends mainly on the particle wettability, which is characterized by the interfacial contact angle. When the contact angle lies in the appropriate range (usually 30 < h < 90L) [1,3,30], stable foams can be produced using a variety of techniques, including shaking, stirring, bubbling and microfluidics [12,31,32]. However, only few reports are available on particle-stabilized non-aqueous/oil foams, consisting mainly of low-surface energy particles bearing fluorocarbon chains. This limited scope arises from the low surface tension of organic liquids, restricting particle adsorption at the gas–liquid interface [1]. As proof of concept, Binks and coworkers investigated the foaming behavior of different types of fluorinated particles in non-polar hydrocarbons and polar organic solvents [8,33–35]. The authors demonstrated that particle wettability can be easily adjusted by tuning the degree of fluorination, and in this way suitable contact angles for non-aqueous foam production could be achieved. Besides fluorinated particles, silica particles modified with dichlorodimethylsilane were used by Dyab et al. to stabilize organic foams in glycerine and ethylene glycol [36]. However, the surface tension of both polar organic solvents is relatively high (c > 47 mN m ^{1}), limiting the scope of application. Overall, halo-genated materials may become solid pollutants as they are resis-tant to degradation under environmental conditions. Therefore, developing novel types of non-halogenated foam stabilizers for organic solvents with tunable contact angles is highly desired.

It is known that molecular ordering of monomeric bricks of homopolymers at the air-solvent interface is conditioned by their relative interaction with the solvent and air. For instance, phenyl groups in poly(phenyl methacrylate) are preferentially solvated by chlorobenzene, while the backbone methyl and methylene groups are exposed to air [37]. Inspired by this observation, we assumed that rationally designed particles with phenyl rings and alkyl chains could assemble at the air–liquid interface, thus stabi-lizing foams based on aromatic solvents. The polymerization of bissilylated organic precursors such as bridged bis(trialkoxysilyl) aryl monomers by the sol–gel process is a convenient route for preparing such particles [38–40]. In this approach, SiAOSAi link-ages in the organosilica particles are replaced by SiAR or SiARASi linkages (where R represents organic groups). These hybrid mate-rials combine the advantages of the silica skeleton (e.g., thermal/mechanical stability and presumed chemical inertness) with the properties of the organic moiety [41–44]. Besides, the chemical and physical properties of the materials (e.g., wettability, flexibil-ity) can be readily tuned by adjusting the nature of bridging organic groups [45–47].

Herein, we synthesized a series of organosilica materials from bridged and non-bridged organosilanes precursors (Scheme 1a,b), which are structurally similar to aromatic solvents (e.g., benzyl alcohol). By adjusting the organic architecture and surface proper-ties of the materials, foams could be prepared in a range of aro-matic solvents by hand shaking and using Ultra-Turrax. The foamability was correlated with the chemical structure of the organosilica particles, and the stability range was investigated as a function of the contact angle and surface tension of the solvents.

2. Materials and methods

2.1. Chemicals

Triethoxyphenylsilane (TEPS, 98%), 1,4-bis(triethoxysilyl) benzene (BTEB, 96%), trimethoxy(propyl)silane (TMPS, 98%), tri-methoxy(hexyl)silane (TMHS, 97%), benzyl alcohol (BZA, 99.5%), benzaldehyde (98%), nitrobenzene (99%), aniline (99%), iodoben-zene (97.5%), pyridine (99%), furfuryl alcohol (98%), m-xylene (99%), ethylene glycol (99.5%), 1,5-pentanediol (98%), perfluorooc-tanoic acid (PFOA, 98%), 1H,1H,2H,2H-perfluorodecyltriethoxysi lane (97%), and 3-mercaptopropyltriethoxysilane (95%) were pur-chased from Beijing J&K Scientific Ltd. 4,4^{0}-bis(triethoxysilyl)-1,1^{0} -biphenyl (BTEBP) was obtained from Fluorochem Ltd. Bis(trime thoxysilylethyl)benzene (BTMEB, 95%) was procured from Gelest Inc. Ethanol (95%), ammonium hydroxide (25–28%), acetophenone (99%), anisole (99%), phenyl acetate (99%), ethylbenzene (98.5%),

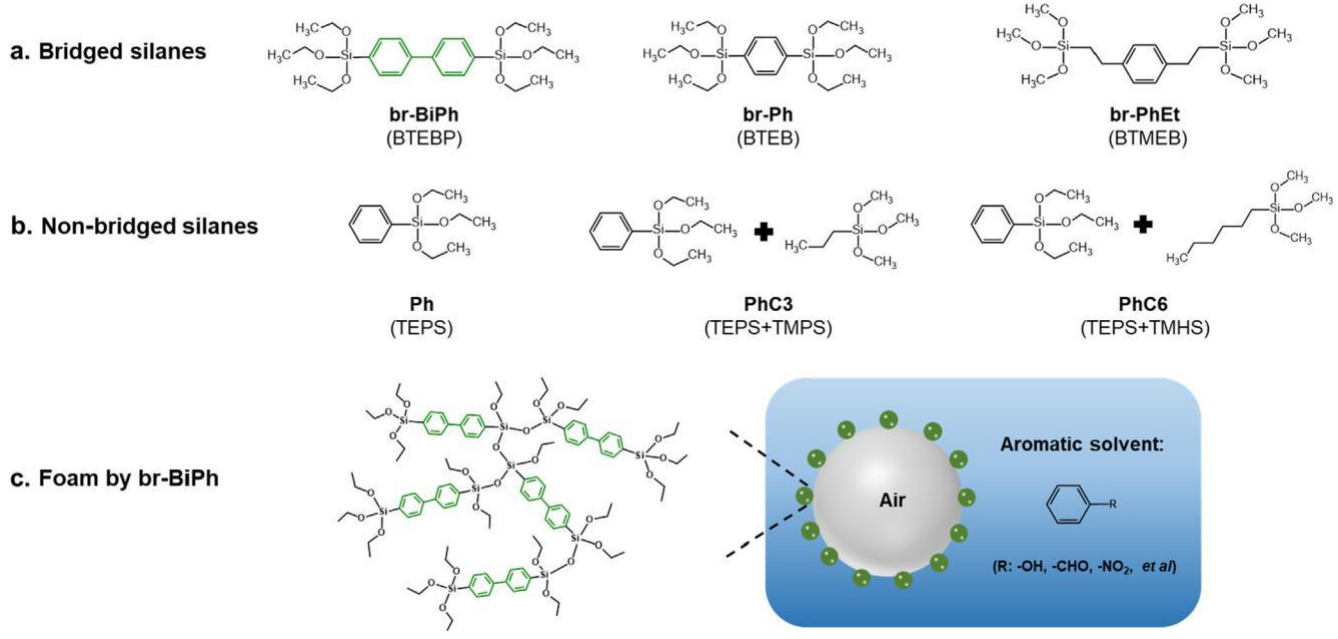

Scheme 1. (a, b) Chemical structure and abbreviations of organosilicas and related precursors; (c) illustration of a bubble stabilized by br-BiPh particles.

toluene (99.5%) and sodium dodecyl sulfate (SDS) were purchased from Sinopharm Chemical Reagent Co., Ltd. Acetone d_6 (99.9 atom %D) was obtained from Adamas-beta. Myristic acid (MA, 99%), sodium dodecylbenzenesulfonate (SDBS) and polystyrene (PS, Mw = 35,000) were purchased from Sigma-Aldrich. Polytetrafluo-roethylene (PTFE, 5 lm particle size) was procured from Aladdin Company.

2.2. Preparation of bridged organosilica particles from bissilylated precursors.

The bridged organosilica particles were synthesized from bissi-lylated organic precursors (Scheme 1) following a modified Stöber method [48]. In a typical synthesis, 1 mL of BTEBP was rapidly added into a mixture of ethanol (12 mL), deionized water (1.6 mL) and NH_3 H_2O (0.5 mL). The mixture was then vigorously stirred at 35 LC for 3 h, resulting in a precipitate. The as-prepared material was isolated by centrifugation and washed three times with ethanol. After drying at 80 LC overnight, biphenyl-bridged particles (denoted as br-BiPh) were obtained. The synthetic proce-dure for phenyl-bridged particles (br-Ph) and phenylethyl-bridged particles (br-PhEt) was similar to that for br-BiPh, except for the substitution of BTEBP with BTEB and BTMEB, respectively.

2.3. Preparation of alkyl-modified organosilicas from phenyltriethoxysilane

Alkyl-modified organosilicas were prepared using tri-ethoxyphenylsilane (TEPS), trimethoxy(propyl)silane (TMPS) and trimethoxy(hexyl)silane (THPS) as co-precursors. For the synthesis of PhC3, 12 mL of ethanol, 1.6 mL of deionized water, and 0.5 mL of NH_3 H_2O were mixed at room temperature. Then, 2 mL of TEPS and 1.5 mL of TMPS were rapidly added and the reaction was left under stirring for 20 h. The final product was obtained after washing with ethanol and drying overnight. For synthesis of PhC6, the volume of mixed precursors was 2 mL of TEPS and 1.9 mL of THPS. Finally, for the synthesis of unmodified organosilicas (Ph), 2 mL of TEPS was used.

2.4. Preparation of fluorinated silica particles

In a typical synthesis, 4 mL of TEOS, 80 mL of ethanol, 11.2 mL of deionized water and 3.2 mL of NH_3 H_2O were mixed at 40 LC for 5 min. Then, a mixture of 1H,1H,2H,2H-perfluorodecyltriethoxysi lane (1.97 mL) and (3-mercaptopropyl)triethoxysilane (0.27 mL) was added under vigorous stirring, and the solution was reacted for 30 min. The solid samples were collected by centrifugation and washed three times with ethanol. After drying at 80 LC over-night, the fluorinated silica particles (SiO_2-F_{17}) were obtained.

2.5. Foaming tests

The non-aqueous foams were first prepared by hand shaking (low energy method). Typically, 2 mL of the given solvent and 20 mg of solid stabilizer (1 wt%) were added into a 4-mL glass vial. After ultrasonication for 10 min, the vial was sealed and vigorously hand shaken for 30 s to generate foams. Foams were also prepared using a high-speed homogenizer (IKA Ultra-Turrax T25 equipped with a S25N-8G dispersing tool). In these tests, a given amount of solid sample was dispersed in 2 mL of solvent, and the disper-sion was aerated at 16,000 rpm for 3 min. The resulting foams were kept static in front of a light board to obtain good contrast and measure the foamability or foam volume at time = 0, and monitor the time-evolution of the foam volume to assess its stability.

The foams obtained with 1 wt% biphenyl-bridged particles were placed on glass microscope slide, and were visualized using an Olympus IX-51 light transmission microscope equipped with 10 ocular, 4 and 10 objectives. Olympus cellSens Standard software was used for bubble size measurements, and ImageJ soft-ware was applied to quantify the size.

2.6. Characterization techniques

Transmission electron microscopy (TEM) was used to investi-gate the morphology of organosilica particles and measure the par-ticle size distributions, using a JEOL JEM-2100 microscope operating at 200 kV. The samples were dispersed in acetone and then deposited on a carbon grid for observation. The particle size distributions were measured using around 100 particles for each sample.

Thermogravimetric analysis (TGA) was carried out on a TA SDT Q600 Instrument by heating the samples from the room tempera-ture to 900 LC at a rate of 10 LC min^{-1} in air.

Fourier-transform infrared (FT-IR) spectra were recorded using a Thermo Scientific Nicolet iS50 equipped with an ATR accessory and operating in the range of 400–4000 cm^{-1}.

^{13}C and ^{29}Si CP-MAS solid-state NMR spectra were recorded on a Bruker AVANCE III 500 MHz spectrometer. ^{13}C and ^{29}Si liquid-state NMR spectra were recorded on a Bruker 600 MHz instrument using acetoned_6 as solvent.

Dynamic light scattering (DLS) measurements were carried out using a Malvern Zetasizer Nano ZS particle size analyzer at 25 LC.

The contact angles were measured at room temperature using the Attension Theta T200 optical tensiometer (Biolin Scientific) equipped with a video capture device. Typically, a drop of solvent was placed on the pellets made by compressing the samples in a 1.3 cm diameter steel die under a pressure of 5 Tons.

The surface tension of organosilica particles was measured in different solvents using a force tensiometer with a platinum Wil-helmy plate (Sigma 700, Biolin Scientific) at 25 LC.

3. Results and discussion

3.1. Characterization of bridged organosilica particles

In order to achieve good foamability in organic solvents, it is key to tune the surface properties of organosilicas by variation of the organic groups incorporated into the network. We synthesized three bridged organosilica particles by sol–gel polycondensation of bissilylated precursors containing phenyl rings. The structural formulas of the starting materials and resulting organosilica parti-cles are presented in Scheme 1a. The TEM images reveal regular spherical shapes for br-BiPh particles with a diameter ranging from 60 to 650 nm (Fig. 1, Figure S1a–f), while the size of br-Ph and br-PhEt particles ~~are~~ fall into the range of 50–210 nm and 25–100 nm (Figure S1g–i), respectively.

TG analysis of the different particles reveals two thermal decomposition steps located in the temperature range 210– 520 LC and 520–700 LC, respectively (Fig. 2a). It is likely that alkyl groups undergo degradation in first step followed by decomposi-tion of phenyl groups. The total weight loss of br-BiPh particles is around 67 wt%. This value is higher than the expected weight loss (59.4 wt%) on the basis of the formula $O_{1.5}Si(C_6H_4)_2SiO_{1.5}$, which can be explained by the presence of non-hydrolyzed ethoxy groups [49]. Both br-Ph and br-PhEt particles exhibit lower weight losses compared to br-BiPh, which is in line with the lower organic con-tent of the precursors.

Fig. 2b shows the FT-IR spectra of bridged organosilica particles. The most prominent band appearing at 1068 cm^{-1} is ascribed to the SiAOASi stretching mode. Characteristic bands belonging to phenyl groups are also visible at 1602 cm^{-1} and 1385 cm^{-1}. More-

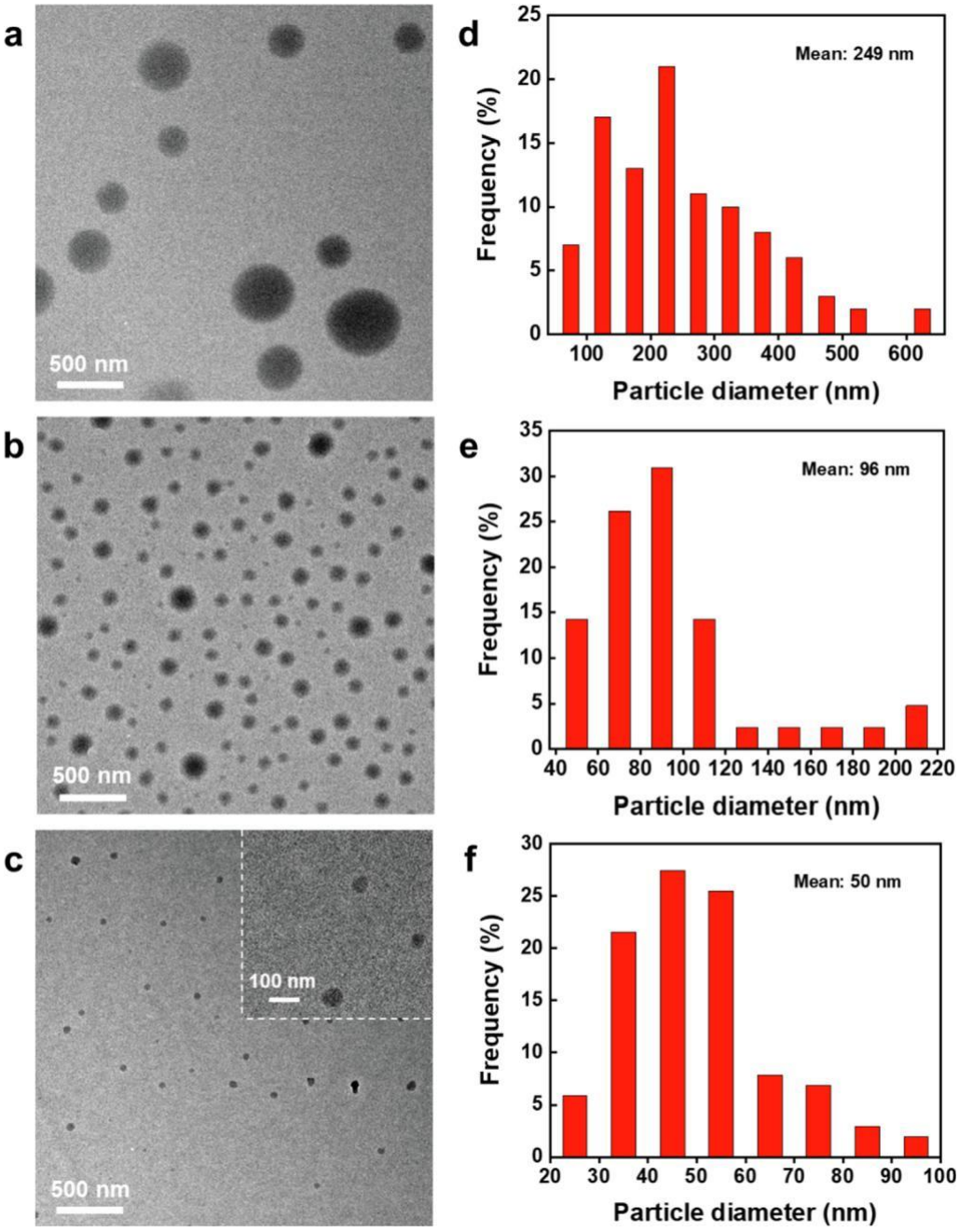

Fig. 1. TEM images of (a) br-BiPh, (b) br-Ph and (c) br-PhEt samples and (b, d, f) corresponding particle size distribution (computed using around 100 particles).

over, several bands appear in the range 2800–3000 cm ^{1} that can be ascribed to CAH stretching and bending modes, confirming the presence of alkyl chains in br-BiPh particles [50].

Solid-state ^{13}C NMR confirms the presence of a large amount of non-hydrolyzed ethoxy groups (resonance at 58 ppm) in the br-BiPh and br-Ph samples (Fig. 3a), which explains the additional mass loss observed in the TG profiles of the particles. The ^{13}C MAS NMR spectra display four aromatic resonances including two intense signals at 126.6 ppm and 135.6 ppm that can be assigned to carbon atoms in positions 2 and 3 bonded to hydrogen, and substituted carbons in positions 1 and 4 of biphenyl (143.1 and 130.7 ppm) [51–53].

The ^{29}Si MAS NMR spectrum of br-BiPh exhibits two signals at 61.52 ppm and 79.74 ppm (Fig. 3c). The former signal can be attributed to T^0 [$CSi(OC_2H_5)_3$] silicon resonances by comparison with the spectrum of the precursor. A similar assignment can be made for br-Ph particles [38,51,54]. The presence of dominant T^0 silicon species further confirms the existence of ethoxy groups in br-BiPh and br-Ph. In contrast, br-PhEt displays a relatively weak signal corresponding to T^0 silicon species centered at 45.86 ppm.

3.2. Foamability studies of bridged organosilica particles

The foamability of the as-prepared bridged organosilica parti-cles was first studied in benzyl alcohol (C = 39.5 mN m ^{1}) by hand shaking. As shown in Fig. 4a and Figure S2, organic foams can be generated from 1 wt% br-BiPh dispersions with a lifetime longer than 1 h, while no foaming occurs for br-Ph and br-PhEt disper-sions. These results point out that the presence of biphenyl rings in br-BiPh particles is crucial for foamability. In addition, we stud-

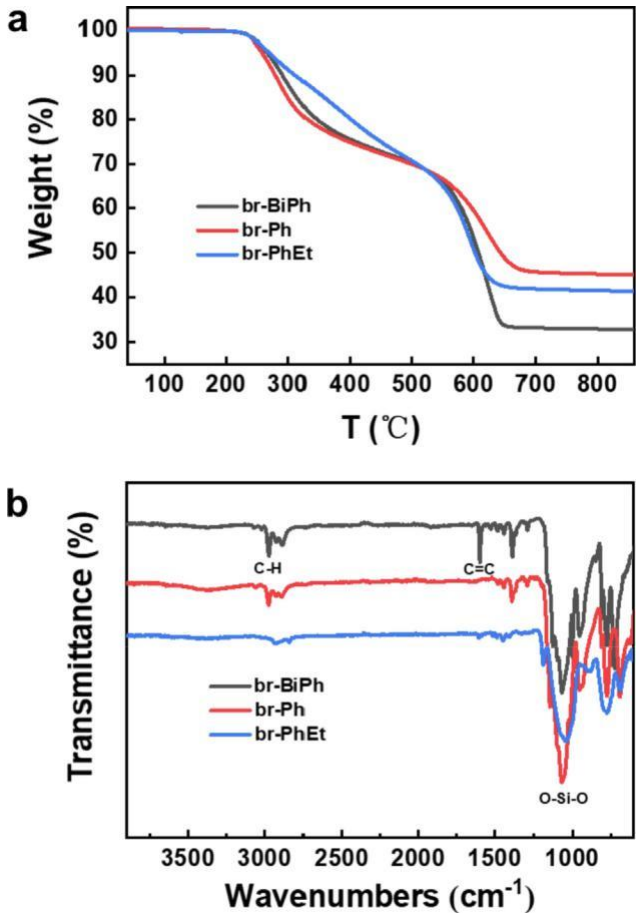

Fig. 2. TG profiles and FT-IR spectra of bridged organosilica particles.

ied the foaming properties of bridged organosilane precursor (BTEBP) used for the preparation of br-BiPh particles (Figure S3). Only a small volume of foams could be produced in benzyl alcohol and the foam lifetime is very short (30 s), indicating that the organic precursor is a bad foaming agent.

Fig. 4b displays optical microscope images of bubbles in benzyl alcohol stabilized by 1 wt% br-BiPh particles. The bubbles are spherical and polydisperse in size with diameters between 60 and 250 lm. The genesis of spherical instead of polyhedral shapes can be explained by the high liquid fraction, u, used. When u is lower than 0.05, bubbles are polyhedral and separated by very thin films, which can be called dry foam [55,56]. For particle-stabilized foams, non-spherical bubbles are favored when particles are den-sely packed at the gas–liquid interface forming a rigid ‘armor’ (high particle loading), preventing bubble relaxation to the more stable spherical shape. As u increases, the bubbles become round and approach to spherical geometry, generating a sub- or single mono-layer of particles (low particle loading). When u is higher than ca. 0.36, the foam system enters ‘‘bubbly liquid” state, where the bub-bles are spherical and isolated without contact with neighbors [57,58].

To rationalize the difference in foaming properties, we mea-sured the contact angle of benzyl alcohol on pellets composed of compressed particles. It can be seen from Fig. 4c that br-Ph and br-PhEt samples are fully wetted by benzyl alcohol explaining the non-foaming behavior of these particles. In contrast, the con-tact angle for br-BiPh particles is 53L, which is suitable for foam generation [1,3]. DLS analysis was used to gain insight into the par-ticle size distribution of bridged organosilicas in benzyl alcohol. As shown in Figure S4, br-BiPh particles exhibit one peak centered at 200 nm, demonstrating that they can be well dispersed in benzyl alcohol. However, the particle sizes measured by DLS for br-Ph and br-PhEt are around 400 nm and 700 nm, respectively, which are larger than the values measured by TEM. This discrepancy is attributed to the aggregation of the latter particles in benzyl alco-hol (Figure S5). The adsorption kinetics of such large aggregates is expected to be slow, which may further explain the lack of foama-bility for br-Ph and br-PhEt dispersions.

In order to understand the role of residual ethoxy groups in br-BiPh particles on the foaming properties, we performed a simple hydrolysis test under alkaline conditions (Figure S6). The br-BiPh particles with ethoxy groups are fully hydrolyzed by NH_3 H_2O after continuous stirring for 3 days, and are unable to foam in benzyl alcohol by hand shaking as they are completely wetted by the sol-vent (Figure S7), while non-hydrolyzed br-BiPh particles retain their foamability. These results point out that the presence of ethoxy side chains in the particle structure, with affinity to the gas phase, is crucial for foam formation.

To further explore the role of ethoxy groups (short alkyl chains) in the foaming performance of biphenyl-bridged particles, we pre-pared a series of organosilicas containing phenyl groups and alkyl chains with different length using alkyltrimethoxysilanes and phenyltriethoxysilane as co-precursors. The presence of alkyl chains in the samples was confirmed by TGA and ^{13}C MAS NMR (Figure S8-S9). The foamability of the particles was evaluated in benzyl alcohol both by hand shaking and using Ultra-Turrax. The Ph sample with no side chains is completely wetted by the solvent (Figure S10) and does not foam (Figure S11-S12). Foams can be generated by PhC3 particles, but collapse completely after 1 min most likely due to the low contact angle (38L). Interestingly, the PhC6 sample (with six carbons side chains) shows lower foamabil-ity, even though the contact angle of this sample is closer to that measured for well-foaming br-BiPh particles (46L and 53L, respec-tively). Lower foamability can be explained by the agglomeration of PhC6 particles in benzyl alcohol (Figure S13) and by a simulta-neous increase of the solid–gas and solid–liquid surface tensions with the chain length, making particle adsorption at the interface energetically unfavorable. Accordingly, a chain length of 2–3 car-bons appears to be optimal for the best foaming, which is in good agreement with a previous study [59].

The particle concentration is a well-known parameter control-ling foaming. As shown in Fig. 5a, the initial foam volume after hand shaking increases progressively with the br-BiPh concentra-tion. A similar foam decay rate is observed for 0.5 and 1 wt% of par-ticles (Fig. 5b), and the half-life time (the time required for the foam height to decrease to half its original value) is above 30 min. Foam collapse is faster at 0.1 wt% since a smaller interfacial area can be covered. Catastrophic foam collapse after 30 min is observed at the highest particle concentration (3 wt%), which is likely caused by particle agglomeration [60,61].

Analyzing the properties of foams prepared by hand shaking is sometimes complex because there is limited control on the energy input along the foaming process. To achieve -more controlled energy input, we used Ultra-Turrax T25 equipped with S25N-8G dispersing tool to produce foams. In these tests, a given amount of br-BiPh was dispersed in benzyl alcohol, and the dispersion was aerated at 16,000 rpm for 3 min. At such conditions, organic foams can be generated at higher production rates compared to foams prepared by hand shaking (Fig. 6). For example, the foam volume produced by this high-energy input (V_{foam}/V_{BZA} = 1.34) is much higher than that produced by hand shaking (V_{foam}/ V_{BZA} = 0.42) for 3 wt% of particles. However, the lifetime of foams prepared by Ultra-Turrax is surprisingly shorter, which could be attributed to lower interfacial coverage in the foam system.

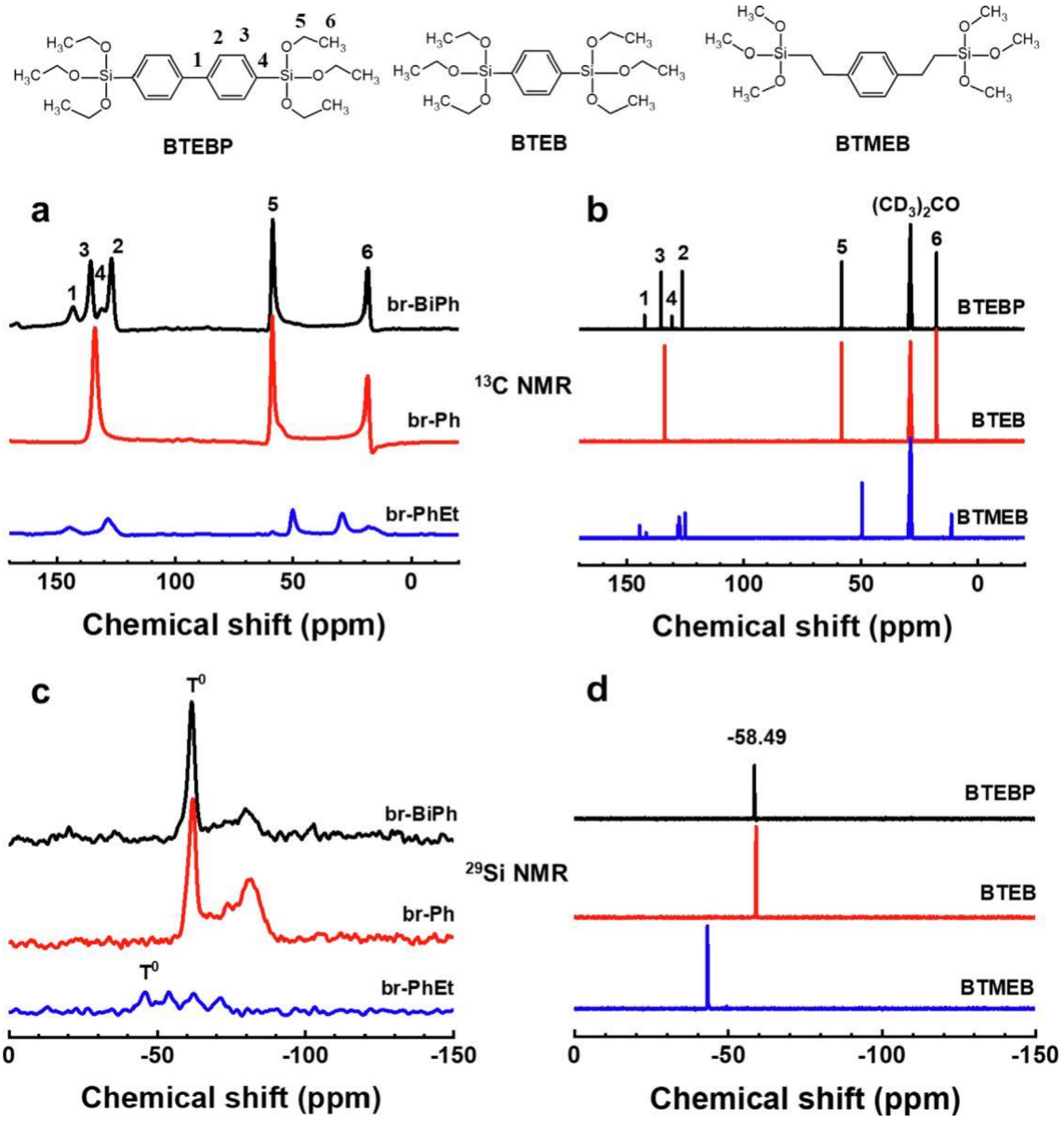

Fig. 3. Solid-state (a) ^{13}C and (c) ^{29}Si CP-MAS NMR spectra of bridged organosilica particles, liquid-state (b) ^{13}C and (d) ^{29}Si NMR spectra of related precursors.

Such high foamability can also be explained by a lower surface tension of the solvent induced by the particles (Figure S14). The surface tension declines from 38.9 to 34.5 mN m ^{1} after addition of 0.1 wt% br-BiPh, with almost no further decrease at higher par-ticle concentration. In contrast, br-Ph and br-PhEt particles exert no effect on the surface tension of benzyl alcohol (Table S1). Unlike surfactants, it is often believed that particles do not affect the foaming properties by significantly reducing the interfacial ten-sion. However, a decrease in surface tension has been reported for some particle-stabilized foams [62,63].

3.3. Effect of the solvent nature on foamability

In addition to the chemical structure and related surface prop-erties of the organosilica particles discussed above, the solvent properties can govern foam generation. To elucidate how the sol-vent affects the particle foamability, we performed hand-shaking tests using a br-BiPh dispersion (1 wt%) in fifteen organic solvents with variable surface tension and functional groups (Table S2).

Stable non-aqueous foams are formed in aromatic solvents with a surface tension between ca. 35 and 44 mN m ^{1} (Fig. 7, Fig-ure S15a). In terms of contact angle, organic foams are generated in the range between 32L and 53L (Figure S16), which is consistent with previous reports [1,3].

Non-polar aromatic solvents with low surface tension (c- < 30 mN m ^{1}), such as toluene, xylene and ethylbenzene, overwet the particles (contact angle 24-25L), resulting in no foam forma-tion. No foams are either obtained for polar aliphatic alcohols like 1,5-pentanediol and ethylene glycol (Figure S15b), which are not compatible with br-BiPh particles containing aromatic rings. The former solvent is an interesting example as the surface tension of 1,5-pentanediol is similar to that of well-foaming nitrobenzene and aniline (43.3 vs 43.9 and 43.4 mN m ^{1}, respectively), but the contact angle is much higher (66L vs 45L and 52L, respectively). From Young's equation (eq. (1)) we can derive that the solid–liquid surface tension, c_{sl}, in this solvent is higher than that in nitroben-zene and aniline, as the solid-air surface tension, c_{sa}, is constant and the liquid–air surface tension c_{la}, is nearly identical for all

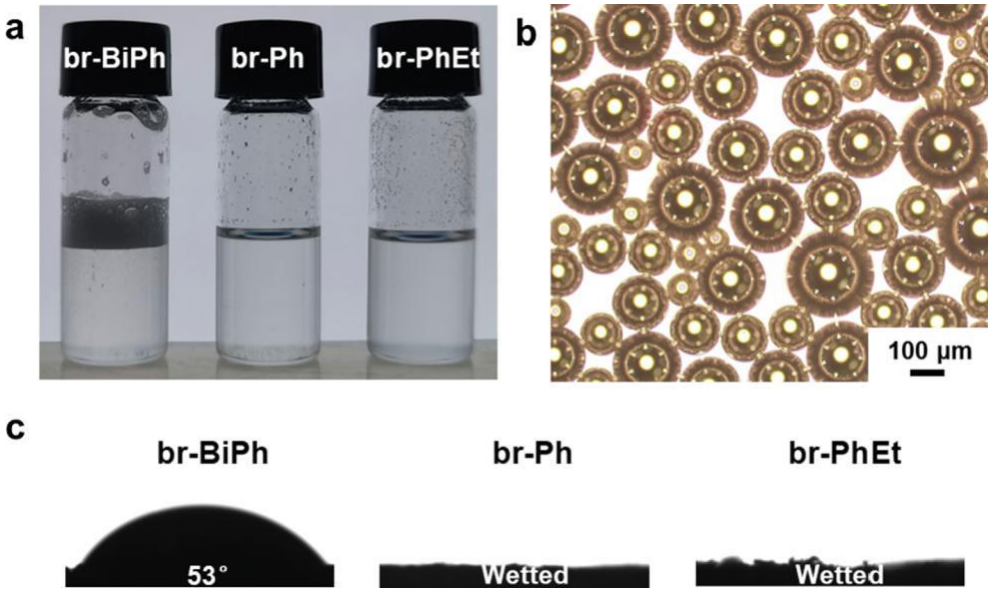

Fig. 4. (a) Foamability of 1 wt% bridged organosilica particles in benzyl alcohol after hand shaking (with backlight), (b) optical microscopy images of bubbles stabilized by 1 wt% br-BiPh, (c) contact angles of br-BiPh, br-Ph and br-PhEt with benzyl alcohol.

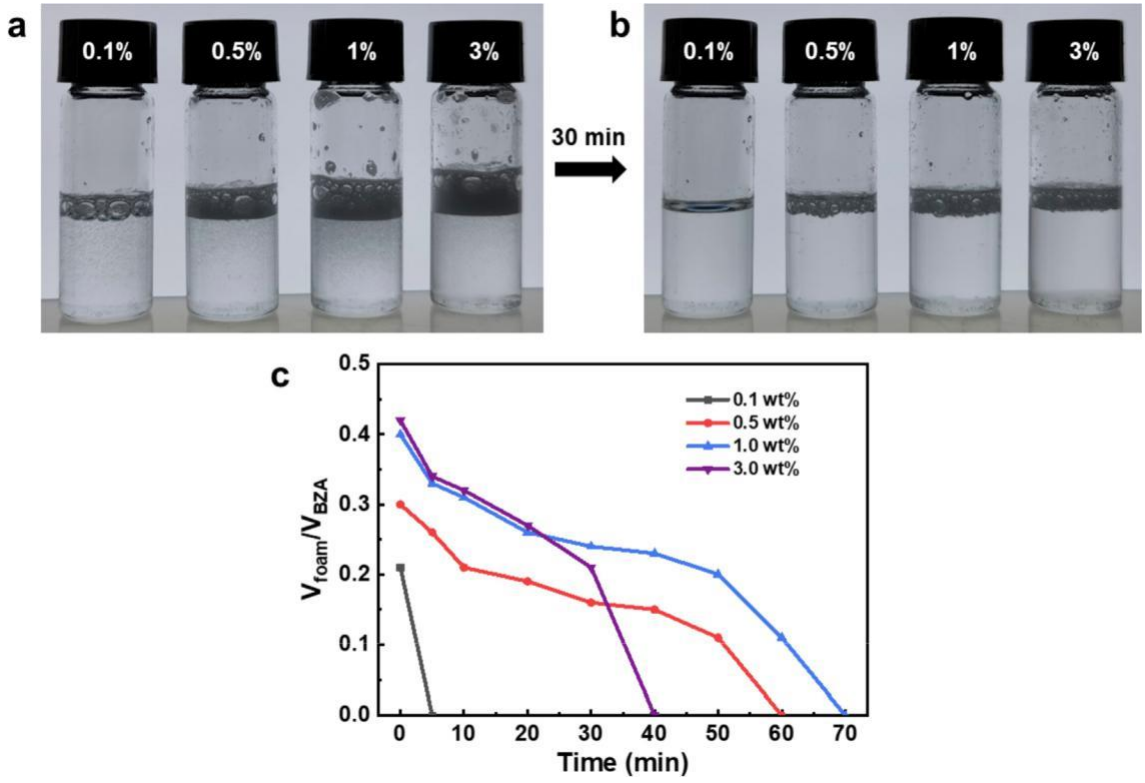

Fig. 5. Images of foams stabilized by br-BiPh with different particle fractions taken (a) immediately after hand shaking and (b) after 30 min, and (c) time-evolution of foam volume. V_{foam}/V_{BZA} = foam volume/volume of benzyl alcohol (‘‘foamability”).

three solvents. Bad wetting of the particles by 1,5-pentanediol therefore renders the thermodynamic condition of particle adsorp-tion at the interface (eq. (2)) invalid, preventing foam formation.

$$\cos h = \frac{c_{sa} - c_{sl}}{c_{la}} \quad \text{ð1Þ}$$

$$c_{sa} + c_{sl} < c_{la} \quad \text{ð2Þ}$$

Overall, from the above analysis, br-BiPh particles promote the foamability for aromatic solvents with substituents including het-eroatoms. Although no clear correlation can be established between the foamability and the nature of the substituent, the presence of strong electron-withdrawing groups in the benzene ring (e.g., nitro, iodo) appears to favour foam generation.

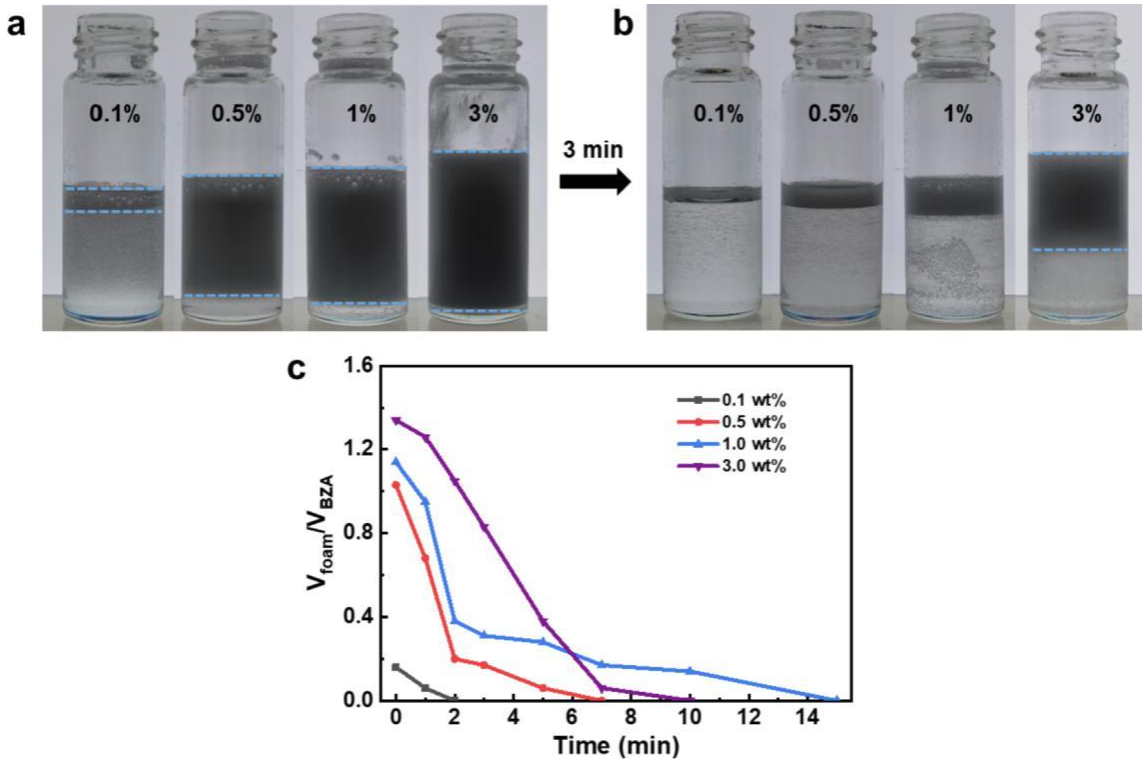

Fig. 6. Representative images of foams produced by Ultra-Turrax at various br-BiPh concentrations taken (a) immediately after preparation and (b) after 3 min, and (c) time-evolution of foam volume.

3.4. Comparison of foams stabilized by different particles and surfactants

In pioneering studies, polytetrafluoroethylene (PTFE) and fluorinated particles have been used as foaming agents to stabilize foams based on apolar aromatic solvents (e.g., toluene, benzene, benzyl acetate) [33,34,64]. Nevertheless, very few studies has been reported on the stabilization of non-aqueous foams based on aromatic solvents with relatively high polarity (e.g., benzyl alcohol, aniline). In this section, the advantages and drawbacks of reported stabilizers is discussed and compared with the foaming properties of br-BiPh particles (Table 1). As shown in Fig. 8a, only br-BiPh particles and fluorinated surfactants (PFOA) afford good foamability, which can be explained by a decrease of the surface tension of benzyl alcohol (Table S1). However, foam stability with PFOA is much lower (1 min) compared to that with br-BiPh particles (70 min), and it is difficult to efficiently separate and recycle surfactants from the systems.

We also studied the foaming properties of br-BiPh particles at higher temperature (80 LC). The particles maintain good foamability in benzyl alcohol, even though the foam lifetime is shortened (40 min, Fig. 8b), pointing out a broad foaming temperature window. On the contrary, for oil foams stabilized by long-chain fatty acid esters or fatty acid crystals in vegetable oils, the solid phase will melt at this temperature and become a homogeneous liquid phase, and no foam will remain [22,65–67]. As a typical example of fatty acid crystals, myristic acid (MA) can enable foam formation in high oleic sunflower oil at room temperature [66]. However, in our case, almost no foams can be generated in benzyl alcohol both at room temperature and high temperature (Fig. 8).

In the case of other fluorinated stabilizers, there exists no surface tension effect in the presence of PTFE and fluorinated silica particles (38.8 and 39.0 mN m ^{1}, respectively), thus no foam formation is observed for benzyl alcohol (Fig. 8a). In addition, fluori-

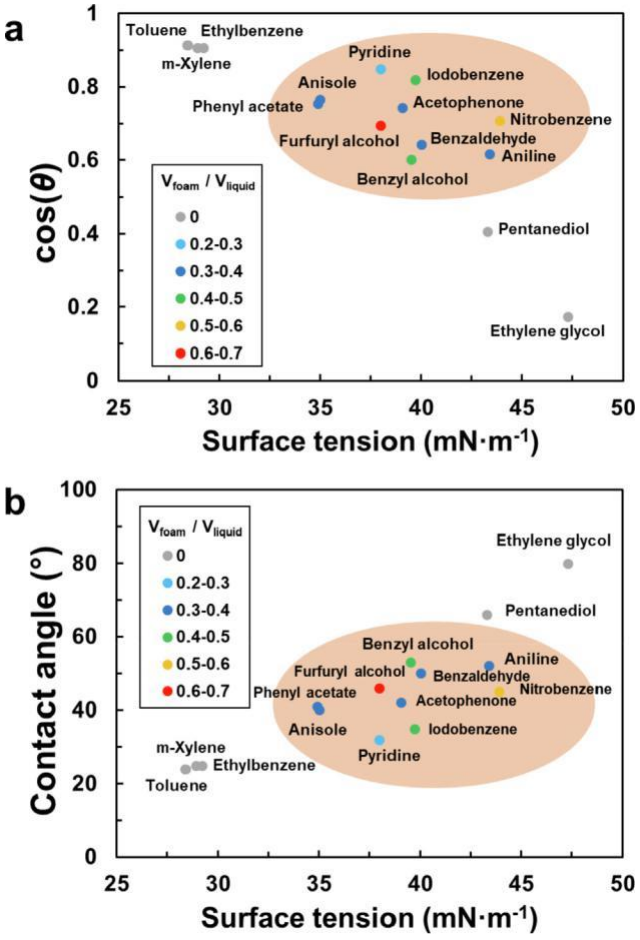

Fig. 7. Cosine of contact angle (a) and contact angle (b) of solvent on br-BiPh as a function of the solvent surface tension.

Table 1
Comparison of non-aqueous foams between br-BiPh particles and other foaming agents.

Entry	Additive	Non-aqueous systems	Advantages	Drawbacks	Ref.
1	br-BiPh particles	Aromatic solvents with surface tension in the range 35 and 44 mN m^{-1}	Thermal stability up to 210 LC, good foamability by hand shaking and outstanding foamability with ultra-turrax	Easily hydrolyzed under acid/alkaline conditions, low foam stability with ultra-turrax	This work
2	PTFE and oligomeric tetrafluoroethylene (OTFE)	Peanut oil, sunflower oil, rapeseed oil, eugenol, tricresyl phosphate, ahexyl cinnamaldehyde, benzyl acetate, bromonaphthalene, few bubbles in benzene	Outstanding chemical and thermal stability	Highly resistant to environmental degradation, poor dispersibility in the solvent.	[27,34,64]
3	Fluorinated particles (silica, sericite, clays and zinc oxide)	Oils with surface tension > 26 mN m^{-1} (e.g., sunflower oil, toluene, benzene, benzyl acetate. hexadecane)	Oil marbles and foams can be obtained by varying the degree of fluorination	Resistant to degrade under environmental conditions	[8,33,35,68]
4	Specialty surfactants (e.g. fluoroalkyl ester)	Dodecane, polyurethane	Soluble in liquid, aggregation and sedimentation unlikely to occur	Difficult to remove or recycle from the oils	[24,69]
5	Surfactant crystals (e.g. fatty acid ester and myristic acid crystals)	Vegetable oils (e.g., olive oil, sunflower oil, squalane, liquid paraffin)	Naturally abundant, low cost	Foams in limited oils, solubilize at elevated temperature	[22,65–67]
6	Asphaltenes and resins	Crude oil	Naturally occurring compounds in crude oil	Only foams in crude oil and synthetic crude oil	[25,70]

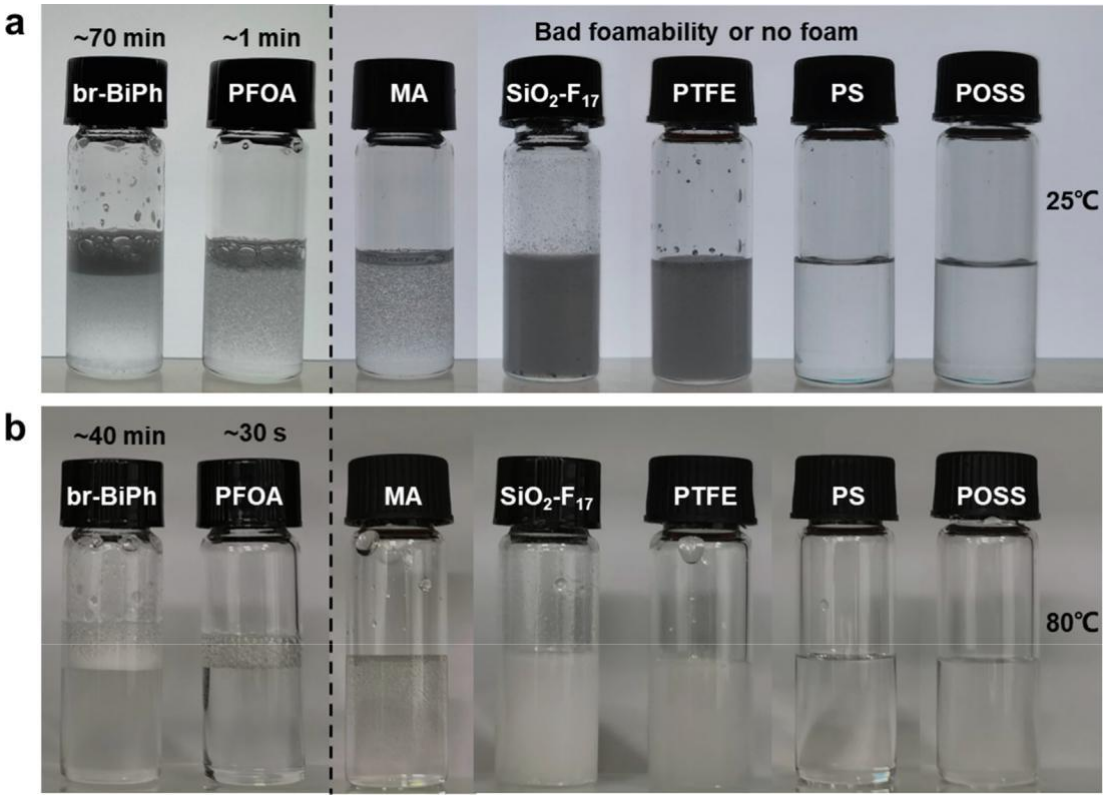

Fig. 8. Foamability of benzyl alcohol in the presence of different particles and surfactants (1 wt%) at (a) room temperature and (b) 80 LC.

nated silica particles with different fluorine content are not surface active for benzyl alcohol [33]. Commercial polymers containing benzene rings (e.g., polystyrene) cannot stabilize foams in benzyl alcohol, most likely due to the absence of alkyl chains. Based on these studies, it can be concluded that br-BiPh particles exhibit better foaming properties (higher foamability and stability) for benzyl alcohol compared to conventional fluorinated particles and surfactants.

4. Conclusions

In this paper, we presented one of the rare examples of non-fluorinated particles stabilizing foams in organic solvents. Biphenyl-bridged particles could adsorb at the air-solvent inter-face, lowering the solvent surface tension and hence facilitating the generation of high-volume foams in benzyl alcohol. The foams produced by hand shaking have a lifetime longer than 1 h. In con-

trast, polytetrafluoroethylene [34,64], myristic acid [66] reported in previous studies, and other fluorinated stabilizers, were unable to generate foams or exhibited very short foam lifetime (ca. 1 min).

The particle structure was directly related to such good foama-bility: both the presence of biphenyl rings (mimicking the struc-ture of the solvent) and short alkyl side chains (ethoxy groups, wetted by the gas phase) was essential to ensure good foaming, confirming our initial hypothesis. The alkyl chains should be about 2–3 carbon long: longer chains prevented foam formation, whereas the absence of side chains led to particle overwetting by the sol-vent. The contact angle was a key parameter controlling foaming. Foams were generated in the contact angle range between 32L and 53L, with a maximum foamability around 45L. In the mean-time, the surface tension of the solvent should lie in the range 35–44 mN m ^{1}.

Overall, this study delivers better understanding of organic foams stabilized by colloidal particles, which can help the formula-tion of innovative products and control industrial processes, and opens perspectives for the synthesis of new non-fluorinated foam-ing materials.

CRediT authorship contribution statement

Andong Feng: Investigation, Writing – original draft. Dmytro Dedovets: Conceptualization, Methodology, Data curation, Writing – review & editing. Yunjiao Gu: Methodology, Validation, Supervi-sion. Shi Zhang: Validation. Jin Sha: Investigation. Xia Han: Inves-tigation, Resources. Marc Pera-Titus: Conceptualization, Writing – review & editing, Supervision, Project administration, Funding acquisition.

Declaration of Competing Interest

The authors declare that they have no known competing finan-cial interests or personal relationships that could have appeared to influence the work reported in this paper.

Acknowledgements

The project was funded by the ERC grant Michelangelo (ref. 771586).

Appendix A. Supplementary material

References

[1] A.-L. Fameau, A. Saint-Jalmes, Non-aqueous foams: Current understanding on the formation and stability mechanisms, Adv. Colloid Interface Sci. 247 (2017) 454–464.

[2] J.A. Rodrigues, E. Rio, J. Bobroff, D. Langevin, W. Drenckhan, Generation and manipulation of bubbles and foams stabilised by magnetic nanoparticles, Colloids Surf., A 384 (1-3) (2011) 408–416.

[3] B.P. Binks, B. Vishal, Particle-stabilized oil foams, Adv. Colloid Interface Sci. 291 (2021) 102404, https://doi.org/10.1016/j.cis.2021.102404.

[4] B.P. Binks, H. Shi, Aqueous foams in the presence of surfactant crystals, Langmuir 36 (4) (2020) 991–1002.

[5] Y. Sheng, K. Lin, B.P. Binks, T.o. Ngai, Ultra-stable aqueous foams induced by interfacial co-assembly of highly hydrophobic particles and hydrophilic polymer, J. Colloid Interface Sci. 579 (2020) 628–636.

[6] M. Safouane, D. Langevin, B.P. Binks, Effect of particle hydrophobicity on the properties of silica particle layers at the air water interface, Langmuir 23 (23) (2007) 11546–11553.

[7] B.P. Binks, T.S. Horozov, Aqueous foams stabilized solely by silica nanoparticles, Angew. Chem. Int. Ed. 44 (24) (2005) 3722–3725.

[8] B.P. Binks, T. Sekine, A.T. Tyowua, Dry oil powders and oil foams stabilised by fluorinated clay platelet particles, Soft Matter 10 (4) (2014) 578–589.

[9] R. Murakami, S. Kobayashi, M. Okazaki, A. Bismarck, M. Yamamoto, Effects of contact angle and flocculation of particles of oligomer of tetrafluoroethylene on oil foaming, Front. Chem. 6 (2018) 435.

[10] J. Huang, F. Cheng, B.P. Binks, H. Yang, pH-responsive gas–water–solid interface for multiphase catalysis, J. Am. Chem. Soc. 137 (47) (2015) 15015– 15025.

[11] N.G. Vilkova, S.I. Elaneva, P.M. Kruglyakov, S.I. Karakashev, Foam films from hexylamine stabilized by the silica particles, Mendeleev Commun. 21 (6) (2011) 344–345.

[12] L.R. Arriaga, W. Drenckhan, A. Salonen, J.A. Rodrigues, R. Iniguez-Palomares, E. Rio, D. Langevin, On the long-term stability of foams stabilised by mixtures of nano-particles and oppositely charged short chain surfactants, Soft Matter 8 (43) (2012) 11085–11097.

[13] Y. Zhu, J. Jiang, Z. Cui, B.P. Binks, Responsive aqueous foams stabilised by silica nanoparticles hydrophobised in situ with a switchable surfactant, Soft Matter 10 (48) (2014) 9739–9745.

[14] B.P. Binks, T.S. Horozov, Colloidal particles at liquid interfaces, Cambridge University Press, 2006.

[15] R.J. Pugh, Bubble and foam chemistry, Cambridge University Press, 2016.

[16] I. Cantat, S. Cohen-Addad, F. Elias, F. Graner, R. Höhler, O. Pitois, F. Rouyer, A. Saint-Jalmes, Foams: structure and dynamics, OUP Oxford2013.

[17] E. Dickinson, B.P. Binks, T.S. Horozov, in: Colloidal Particles at Liquid Interfaces, Cambridge University Press, Cambridge, 2006, pp. 298–327, https://doi.org/10.1017/CBO9780511536670.009.

[18] A.V. Nguyen, R.J. Pugh, G. Jameson, Collection and attachment of particles by air bubbles in froth flotation, (2006).

[19] N. Yekeen, M.A. Manan, A.K. Idris, E. Padmanabhan, R. Junin, A.M. Samin, A.O. Gbadamosi, I. Oguamah, A comprehensive review of experimental studies of nanoparticles-stabilized foam for enhanced oil recovery, J. Petrol. Sci. Eng. 164 (2018) 43–74.

[20] R. Farajzadeh, A. Andrianov, R. Krastev, G. Hirasaki, W.R. Rossen, Foam–oil interaction in porous media: implications for foam assisted enhanced oil recovery, Adv. Colloid Interface Sci. 183 (2012) 1–13.

[21] R. Heymans, I. Tavernier, S. Danthine, T. Rimaux, P. Van der Meeren, K. Dewettinck, Food-grade monoglyceride oil foams: the effect of tempering on foamability, foam stability and rheological properties, Food Funct. 9 (6) (2018) 3143–3154.

[22] L.K. Shrestha, K. Aramaki, H. Kato, Y. Takase, H. Kunieda, Foaming properties of monoglycerol fatty acid esters in nonpolar oil systems, Langmuir 22 (20) (2006) 8337–8345.

[23] I.D. Robb (Ed.), Specialist Surfactants, Springer Netherlands, Dordrecht, 1996.

[24] V. Bergeron, J.E. Hanssen, F.N. Shoghl, Thin-film forces in hydrocarbon foam films and their application to gas-blocking foams in enhanced oil recovery, Colloids Surf., A 123-124 (1997) 609–622.

[25] F. Bauget, D. Langevin, R. Lenormand, Dynamic surface properties of asphaltenes and resins at the oil–air interface, J. Colloid Interface Sci. 239 (2) (2001) 501–508.

[26] C. Blázquez, E. Emond, S. Schneider, C. Dalmazzone, V. Bergeron, Non-aqueous and crude oil foams, Oil & Gas Science and Technology-Revue d'IFP Energies nouvelles 69 (3) (2014) 467–479.

[27] R. Murakami, A. Bismarck, Particle-Stabilized Materials: Dry Oils and (Polymerized) Non-Aqueous Foams, Adv. Funct. Mater. 20 (5) (2010) 732–737.

[28] L. Wang, Q. Cheng, H. Qin, Z. Li, Z. Lou, J. Lu, J. Zhang, Q. Zhou, Synthesis of silicon carbide nanocrystals from waste polytetrafluoroethylene, Dalton Trans. 46 (9) (2017) 2756–2759.

[29] G.W. Kauffman, P.C. Jurs, Prediction of surface tension, viscosity, and thermal conductivity for common organic solvents using quantitative structure property relationships, J. Chem. Inf. Comput. Sci. 41 (2) (2001) 408–418.

[30] B.P. Binks, Particles as surfactants—similarities and differences, Curr. Opin. Colloid Interface Sci. 7 (1-2) (2002) 21–41.

[31] S.I. Karakashev, O. Ozdemir, M.A. Hampton, A.V. Nguyen, Formation and stability of foams stabilized by fine particles with similar size, contact angle and different shapes, Colloids Surf., A 382 (1-3) (2011) 132–138.

[32] N. Mase, T. Mizumori, Y. Tatemoto, Aerobic copper/TEMPO-catalyzed oxidation of primary alcohols to aldehydes using a microbubble strategy to increase gas concentration in liquid phase reactions, Chem. Commun. 47 (7) (2011) 2086–2088.

[33] B.P. Binks, A.T. Tyowua, Influence of the degree of fluorination on the behaviour of silica particles at air–oil surfaces, Soft Matter 9 (3) (2013) 834– 845.

[34] B.P. Binks, A. Rocher, M. Kirkland, Oil foams stabilised solely by particles, Soft Matter 7 (5) (2011) 1800–1808.

[35] B.P. Binks, S.K. Johnston, T. Sekine, A.T. Tyowua, Particles at oil–air surfaces: powdered oil, liquid oil marbles, and oil foam, ACS Appl. Mater. Interfaces 7 (26) (2015) 14328–14337.

[36] A.K. Dyab, H.N. Al-Haque, Particle-stabilised non-aqueous systems, RSC Adv. 3 (32) (2013) 13101–13105.

[37] J.N. Myers, C. Zhang, C. Chen, Z. Chen, Influence of casting solvent on phenyl ordering at the surface of spin cast polymer thin films, J. Colloid Interface Sci. 423 (2014) 60–66.

[38] K.J. Shea, D.A. Loy, O. Webster, Arylsilsesquioxane gels and related materials. New hybrids of organic and inorganic networks, J. Am. Chem. Soc. 114 (17) (1992) 6700–6710.

[39] R. Ciriminna, A. Fidalgo, V. Pandarus, F. Béland, L.M. Ilharco, M. Pagliaro, The sol–gel route to advanced silica-based materials and recent applications, Chem. Rev. 113 (8) (2013) 6592–6620.

[40] F. Hoffmann, M. Cornelius, J. Morell, M. Fröba, Silica-based mesoporous organic–inorganic hybrid materials, Angew. Chem. Int. Ed. 45 (20) (2006) 3216–3251.

[41] N. Mizoshita, T. Tani, S. Inagaki, Syntheses, properties and applications of periodic mesoporous organosilicas prepared from bridged organosilane precursors, Chem. Soc. Rev. 40 (2) (2011) 789–800.
[42] A.P. Dral, C. Lievens, J.E. ten Elshof, Influence of monomer connectivity, network flexibility, and hydrophobicity on the hydrothermal stability of organosilicas, Langmuir 33 (22) (2017) 5527–5536.
[43] M. Ferré, R. Pleixats, M. Wong Chi Man, X. Cattoën, Recyclable organocatalysts based on hybrid silicas, Green Chem. 18 (4) (2016) 881–922.
[44] A. Zamboulis, N. Moitra, J.J. Moreau, X. Cattoën, M.W.C. Man, Hybrid materials: versatile matrices for supporting homogeneous catalysts, J. Mater. Chem. 20 (42) (2010) 9322–9338.
[45] J.G. Croissant, X. Cattoën, J.-O. Durand, M.W.C. Man, N.M. Khashab, Organosilica hybrid nanomaterials with a high organic content: syntheses and applications of silsesquioxanes, Nanoscale 8 (48) (2016) 19945–19972.
[46] U. Diaz, D. Brunel, A. Corma, Catalysis using multifunctional organosiliceous hybrid materials, Chem. Soc. Rev. 42 (9) (2013) 4083–4097.
[47] J.G. Croissant, X. Cattoën, M. Wong Chi Man, J.-O. Durand, N.M. Khashab, Syntheses and applications of periodic mesoporous organosilica nanoparticles, Nanoscale 7 (48) (2015) 20318–20334.
[48] H. Zou, R. Wang, X. Li, X. Wang, S. Zeng, S. Ding, L.u. Li, Z. Zhang, S. Qiu, An organosilane-directed growth-induced etching strategy for preparing hollow/ yolk–shell mesoporous organosilica nanospheres with perpendicular mesochannels and amphiphilic frameworks, J. Mater. Chem. A 2 (31) (2014) 12403–12412.

[49] Y. Yang, A. Sayari, Molecularly ordered biphenyl-bridged mesoporous organosilica prepared under acidic conditions, Chem. Mater. 19 (17) (2007) 4117–4119.

[50] H. Du, P.D. Hamilton, M.A. Reilly, A. d'Avignon, P. Biswas, N. Ravi, A facile synthesis of highly water-soluble, core–shell organo-silica nanoparticles with controllable size via sol–gel process, J. Colloid Interface Sci. 340 (2) (2009) 202–208.

[51] M.P. Kapoor, Q. Yang, S. Inagaki, Self-assembly of biphenylene-bridged hybrid mesoporous solid with molecular-scale periodicity in the pore walls, J. Am. Chem. Soc. 124 (51) (2002) 15176–15177.
[52] M. Park, S.S. Park, M. Selvaraj, D. Zhao, C.-S. Ha, Hydrophobic mesoporous materials for immobilization of enzymes, Microporous Mesoporous Mater. 124 (1-3) (2009) 76–83.

[53] S. Theivendran, J. Zhang, C. Tang, M. Kalantari, Z. Gu, Y. Yang, Y. Yang, E. Strounina, A. Du, C. Yu, Synthesis of biphenyl bridged dendritic mesoporous organosilica with extremely high adsorption of pyrene, J. Mater. Chem. A 7 (19) (2019) 12029–12037.

[54] Y. Yang, A. Sayari, Mesoporous Organosilicates from Multiple Precursors: Co-Condensation or Phase Segregation/Separation?, Chem Mater. 20 (9) (2008) 2980–2984.

[55] Y. Furuta, N. Oikawa, R. Kurita, Close relationship between a dry-wet transition and a bubble rearrangement in two-dimensional foam, Sci. Rep. 6 (2016) 37506.

[56] S. Andrieux, A. Quell, C. Stubenrauch, W. Drenckhan, Liquid foam templating– A route to tailor-made polymer foams, Adv. Colloid Interface Sci. 256 (2018) 276–290.

[57] A. Trybala, N. Koursari, P. Johnson, O. Arjmandi-Tash, V. Starov, Interaction of liquid foams with porous substrates, Curr. Opin. Colloid Interface Sci. 39 (2019) 212–219.

[58] W. Drenckhan, D. Langevin, Monodisperse foams in one to three dimensions, Curr. Opin. Colloid Interface Sci. 15 (5) (2010) 341–358.
[59] X. Bai, N. Song, L. Wen, X. Huang, J. Zhang, Y. Zhang, Y. Zhao, Environmentally benign multiphase solid–liquid–gas catalysis, Green Chem. 22 (3) (2020) 895– 902.

[60] N. Yekeen, A.K. Idris, M.A. Manan, A.M. Samin, A.R. Risal, T.X. Kun, Bulk and bubble-scale experimental studies of influence of nanoparticles on foam stability, Chin. J. Chem. Eng. 25 (3) (2017) 347–357.
[61] H. Holthoff, S.U. Egelhaaf, M. Borkovec, P. Schurtenberger, H. Sticher, Coagulation rate measurements of colloidal particles by simultaneous static and dynamic light scattering, Langmuir 12 (23) (1996) 5541–5549.
[62] A. Stocco, W. Drenckhan, E. Rio, D. Langevin, B.P. Binks, Particle-stabilised foams: an interfacial study, Soft Matter 5 (11) (2009) 2215–2222.
[63] T.N. Hunter, R.J. Pugh, G.V. Franks, G.J. Jameson, The role of particles in stabilising foams and emulsions, Adv. Colloid Interface Sci. 137 (2) (2008) 57– 81.

[64] B.P. Binks, A. Rocher, Stabilisation of liquid–air surfaces by particles of low surface energy, PCCP 12 (32) (2010) 9169–9171.
[65] L.K. Shrestha, R.G. Shrestha, S.C. Sharma, K. Aramaki, Stabilization of nonaqueous foam with lamellar liquid crystal particles in diglycerol monolaurate/olive oil system, J. Colloid Interface Sci. 328 (1) (2008) 172–179.
[66] B.P. Binks, E.J. Garvey, J. Vieira, Whipped oil stabilised by surfactant crystals, Chem. Sci. 7 (4) (2016) 2621–2632.
[67] Y.u. Liu, B.P. Binks, Foams of vegetable oils containing long-chain triglycerides, J. Colloid Interface Sci. 583 (2021) 522–534.
[68] Y. Lai, H. Zhou, Z. Zhang, Y. Tang, J.W.C. Ho, J. Huang, Q. Tay, K. Zhang, Z. Chen, B.P. Binks, Multifunctional TiO2-Based Particles: The Effect of Fluorination Degree and Liquid Surface Tension on Wetting Behavior, Part. Part. Syst. Char. 32 (3) (2015) 355–363.
[69] W.R. Rossen, R. Prud'homme, S. Khan, Foams: theory, measurements and applications, Foams in Enhanced Oil Recovery (1996) 413–464.
[70] N.N. Zaki, M.K. Poindexter, P.K. Kilpatrick, Factors contributing to petroleum foaming. 2. Synthetic crude oil systems, Energy Fuels 16 (3) (2002) 711–717.